Electronic Supplementary Material

Bio-Ionic Liquid based Self Healable and Adhesive Ionic Hydrogel for the On-demand Transdermal Delivery of Chemotherapeutic Drug

Raviraj Pansuriya[a], James Doutch[b], Bhagyesh Parmar[a], Suresh Kumar Kailasa[a], Najet Mahmoudi[b]*, Clare Hoskins[c]*, Naved I. Malek[a]*

[a]Ionic Liquids Research Laboratory, Department of Chemistry, Sardar Vallabhbhai National Institute of Technology, Surat-395007, Gujarat, India

[b]ISIS Pulsed Neutron & Muon Source, STFC Rutherford Appleton Laboratory, Harwell Campus, Didcot, OX11 0QX, United Kingdom

[c]Technology and Innovation Centre, Department of Pure and Applied Chemistry, University of Strathclyde, Glasgow G1 1RD, UK

Mechanism for the Formation of Ionic Hydrogel

Ionic hydrogel was prepared by simple, drop wise addition of OA in aqueous solution of [Cho][Gly]. Here, [Cho][Gly] contain positively charged -NMe_3 whereas OA carries a negatively charged carbolxylic -COO group that contributed to the hydrogel formation through electrostatic interaction. From the computational simulations we have confirmed that there is a significant change in the electronic charge distribution around the individual moieities before and after interacting with each other **(Figure 4)**. In detail, there is a significant change in the negative charge distribution around the acid group of standalone OA[1] in regard with the OA interacting with the amine head group of the [Cho][Gly] **(Figure 4a)**. Also, we can observe the changes in the positive charge distribution around the amine head of the [Cho][Gly]. This significant change in the charge distribution leads to a change in the behaviour of OA and [Cho][Gly] that in turn leads to changes in the shape of the aggregates from ellipsoidal to cylindrical to ionic hydrogel, SANS data. Further, the hydrogeln bonding between the [Cho][Gly] and OA was also responsible for the formation of ionic hydrogel, FTIR results. These non-covalent interactions are confirmed thourgh the change in the frequencies of the respective functional groups through FTIR and supported by the NCI analysis as well as the MESP calculations. The non-covalent interactions present between the molecules leads to the transition of the aggregtes structure from ellipsoidal micelles to

cylindrical micelles to worm-like micelles to ionic hydrogel, as shown by SANS analysis. The process of hydrogel formation is influenced by various factors, such as the concentration of OA and pH of the system, and is important for understanding the behavior of the molecules in different contexts.

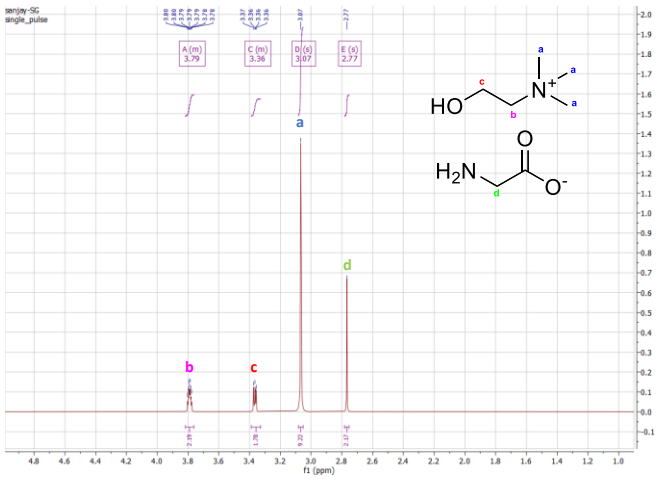

Figure S1: ^{1}H-NMR spectra of [Cho][Gly].

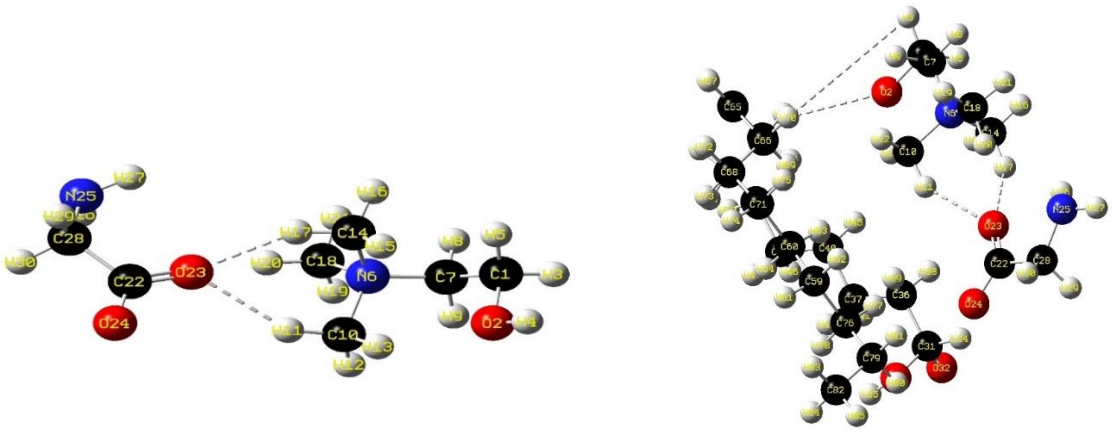

(a) (b)

Figure S2: Optimization structure of (a) [Cho][Gly] and (b) [Cho][Gly]/Oleic acid complex.

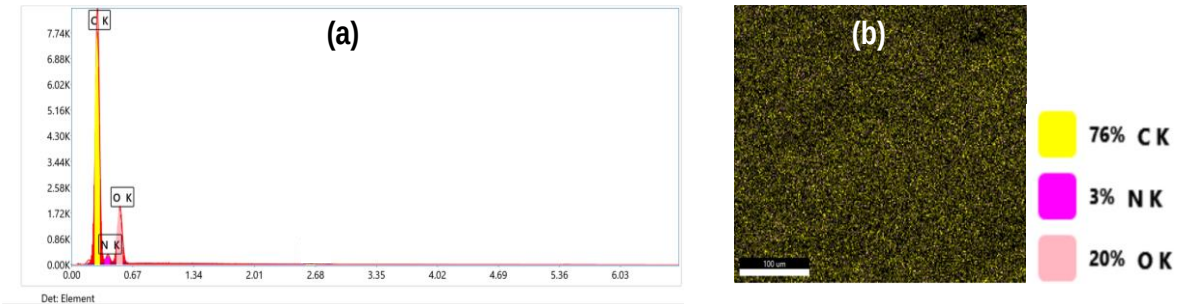

Figure S3: EDX analysis of [Cho][Gly] and OA base ionic hydrogel (a) EDX maping and (b) EDX image.

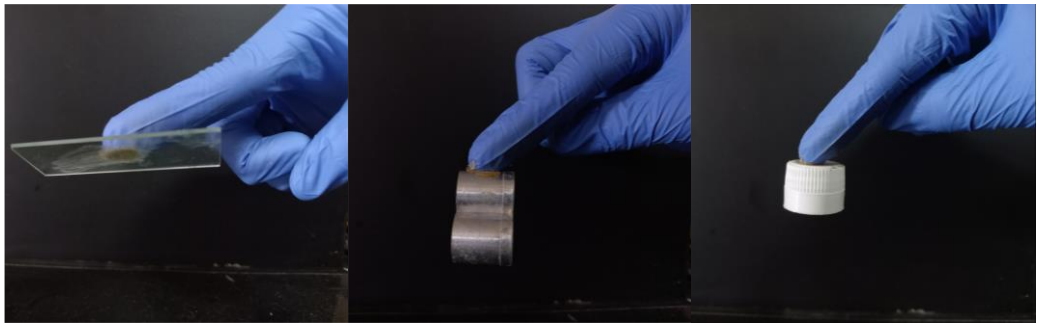

(a)

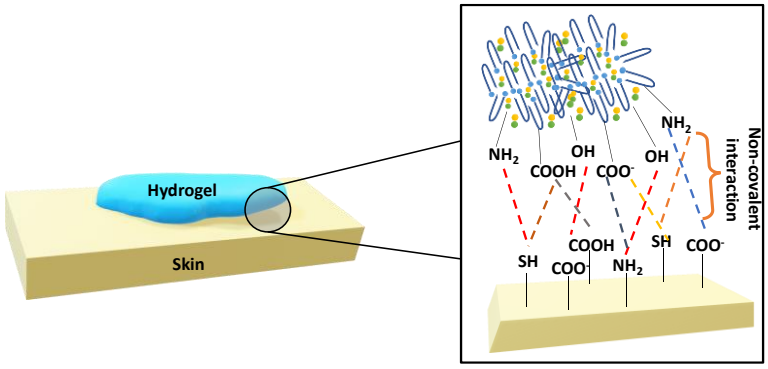

(b)

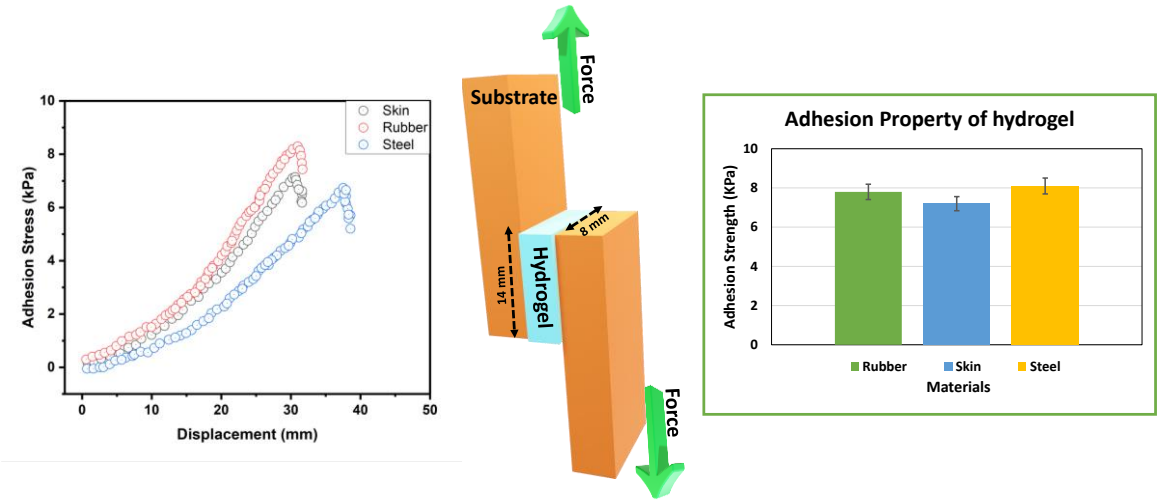

(c)

Figure S4: (a) Visual image of adhesiveness of ionic hydrogel with glass, steel and plastic materials, (b) Graphical representation of interaction between ionic hydrogel and other material (c) Result of lap shear test.

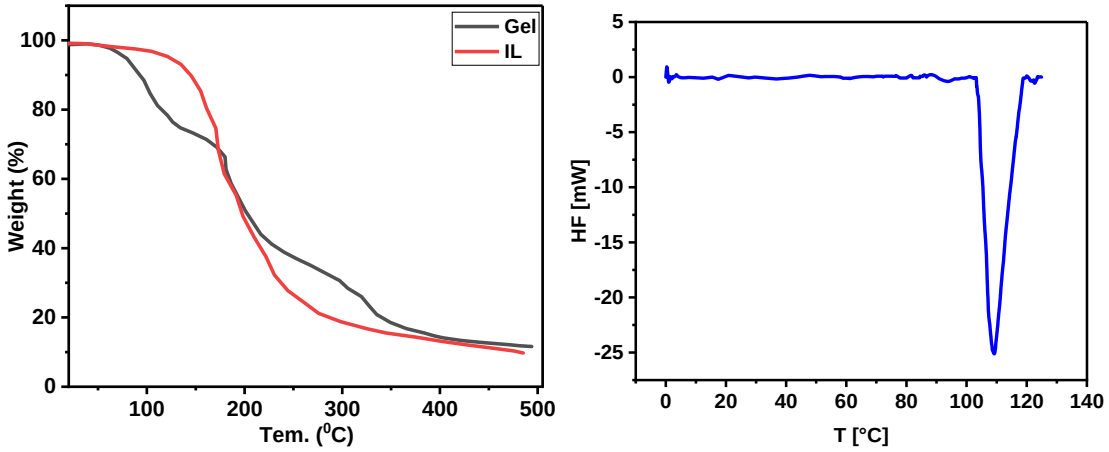

(a) **(b)**

Figure S5: (a) TGA graph of hydrogel, [Cho][Gly]-OA Gel (**Black Line**), [Cho][Gly] (**Red Line**), (b) DSC analysis of hydrogel.

Effect of temperature on the ionic hydrogel

The temperature is the most important stimulus for stimuli-responsive hydrogels, which significantly impacts aggregate size and drug release. We used DLS as a function of temperature to investigate the temperature-responsive behaviour of ionic hydrogel and the effect of temperature on aggregate size. As the temperature of the hydrogel increased from 25 to 75 °C, the average size and PDI value within the hydrogel decreased (**Table S3** and **Figure S6**). The non-covalent interactions within the hydrogel are weakened when the temperature increases, but upon decreasing the temperature, these interactions reform, leading to the gel, transitioning back into its original form (**Figure S6** and **Table S4**).

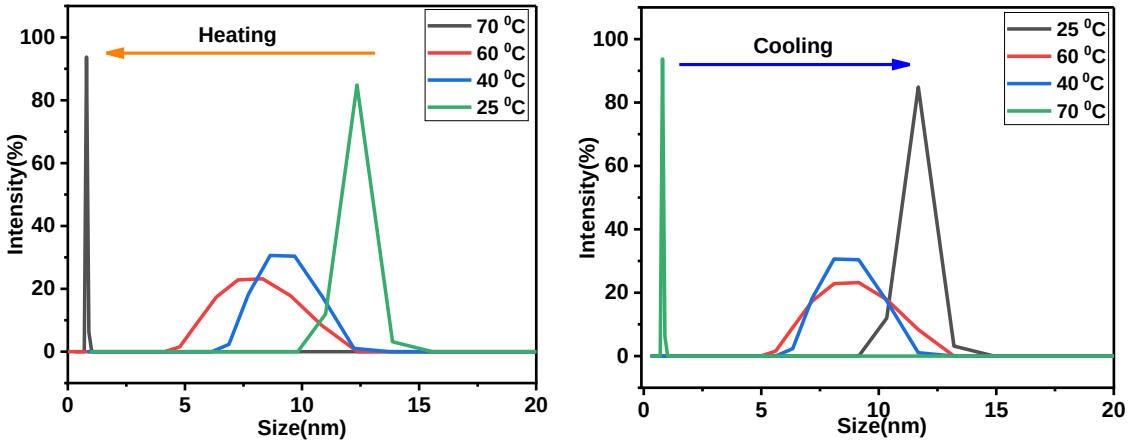

(a) **(b)**

Figure S6: Aggregates size of ionic hydrogel at different temperature measure by DLS analysis, (a) Heating of gel and (b) Cooling of gel.

In vitro drug release

As illustrated in **Figure S7**, 94% of the burst release occurs within 8 hours, observed at pH 2 (gastric condition), attributed to the deformation of the three-dimensional network below pH 5, leading to the release of encapsulated drug molecules. In the case of neutral pH (pH-7.0) condition, 78 % drug was released within 50 h. These findings imply that when utilizing this system orally, adverse effects may be observed in the human body.[2,3] In TDD, drug release is sustained and directed towards the targeted site through the skin, thereby minimizing the

potential side effects associated with TDD-based systems as compared to other ways.

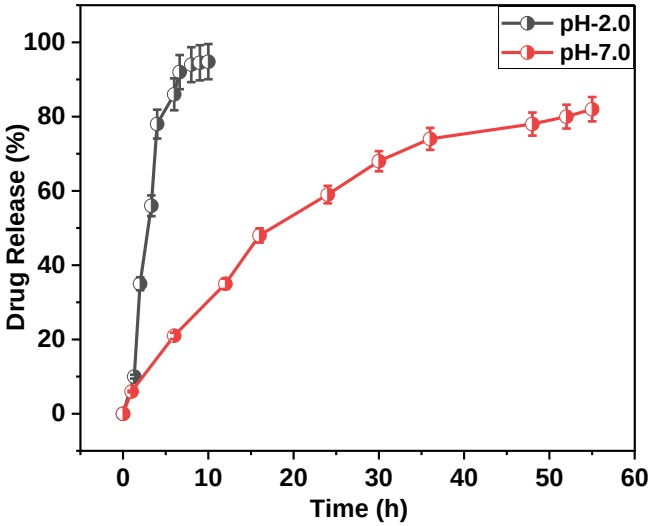

Figure S7: *In vitro* drug release at different pH values.

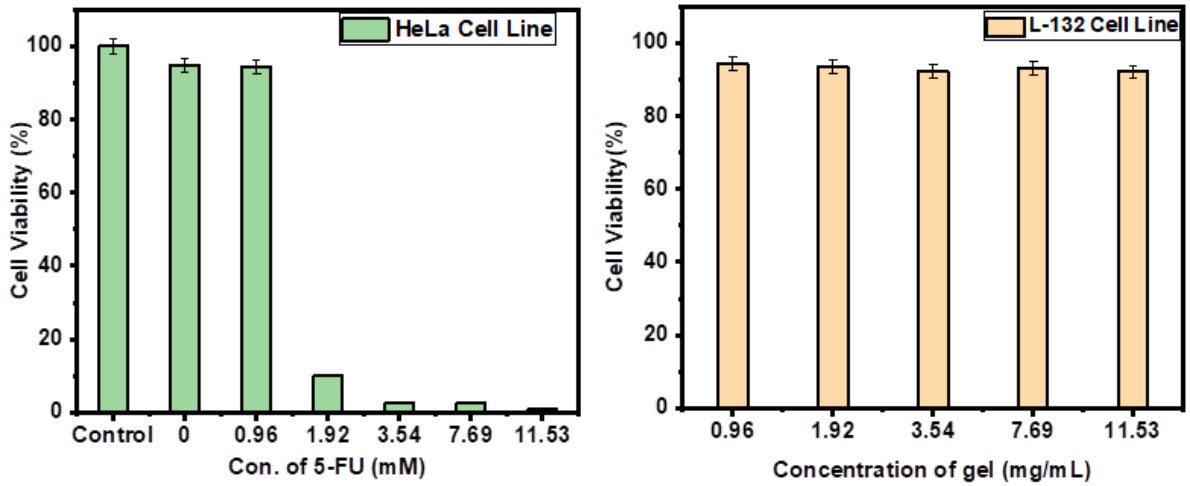

(a) **(b)**

Figure S8: (a)*In vitro* cytotoxicity of drug loaded ionic hydrogel on cervical cancer cell line HeLa cells, (b) *in vitro* biocompatibility of ionic hydrogel on normal cell line L-132 cell.

Tables

Table S1: pH of system when addition of OA in aqueous solution of [Cho][Gly].

[Cho][Gly] (M)	[OA] (M)	pH of system	Nature of system
0.84	0.0	11.12	Solution
0.84	0.15	10.2	Solution
0.84	0.28	8.1	Viscus solution
0.84	0.63	7.5	Loose gel
0.84	0.75	7.0	Ionic Hydrogel

Table S2: Compression of theoretical and practical elemental analysis of gel.

Element present in gel	Theoretical % of element	% of element through EDX
C	72.75	76.00
O	22.64	20.00
N	4.60	3.00

Table S3: Average aggregates size of ionic hydrogel with increases temperature measured by DLS analysis.

Temperature (°C)	Aggregate Size (nm)	PDI
25	11.68	0.21
40	9.15	0.26
60	8.15	0.24
70	0.8	0.12

Table S4: Average aggregates size of ionic hydrogel with decreases temperature measured by DLS analysis.

Temperature (°C)	Aggregate Size (nm)	PDI
70	0.8	0.12
60	7.11	0.21
40	8.50	0.25
25	12.11	0.22

Table S5: Cell viability data of ionic hydrogel with MCF-07 and M-132 Cell lines.

Concentration of gel (mg/mL)	[Cho][Gly]-Gel	
	HaCaT cell line	L-132 cell line
0.96	98.2	94.23
1.92	98.0	93.54
3.54	97.5	92.35
7.69	95.1	93.21
11.53	93.2	92.10

Table S6: FTIR peak shift of SC, after treated with various formulations.

Formulations	**Lipid components of SC**				**Protein components of SC**			
	Absorption CH_2 Asymmetric	**Shift**	**Abs. CH_2 symm.**	**Shift**	**Abs. -C=O Amide**	**Shift**	**Abs. HN-C=O amide**	**shift**
[Cho][Gly]	2920.32	0.09	2850.81	0.02	1644.10	0.8	1539.25	0.05
[Cho][Gly]/OA hydrogel	2926.50	6.27	2857.25	6.46	1648.33	5.03	1545.54	6.3
PBS (Control)	2920.23	-	2850.79	-	1643.35	-	1539.20	-

References

1 S. Mishra, D. Chaturvedi, N. Kumar, P. Tandon and H. W. Siesler, *Chem. Phys. Lipids*, 2010, **163**, 207–217.

2 R. B. Diasio, B. E. Harris, *Clin. Pharmacokinet.* 1989, **16**, 215−37.

3 M. A. Safwat, G. M. Soliman, D. Sayed and M. A. Attia, *Mol. Pharm.*, 2018, **15**, 2194–2205.